

Negative differential conductance in quantum dots in theory and experiment

M. C. Rogge¹, F. Cavaliere^{2,3}, M. Sasseti², R. J. Haug¹, and B. Kramer³

¹*Institut für Festkörperphysik, Universität Hannover, Appelstraße 2, 30167 Hannover, Germany*

²*I. Institut für Theoretische Physik, Universität Hamburg, Jungiusstraße 9, 20355 Hamburg, Germany*

³*INFN-LAMIA, Dipartimento di Fisica Università di Genova, Via Dodecaneso 33, 16146 Genova, Italy*

(Dated: July 17, 2018)

Experimental results for sequential transport through a lateral quantum dot in the regime of spin blockade induced by spin dependent tunneling are compared with theoretical results obtained by solving a master equation for independent electrons. Orbital and spin effects in electron tunneling in the presence of a perpendicular magnetic field are identified and discussed in terms of the Fock-Darwin spectrum with spin. In the nonlinear regime, a regular pattern of negative differential conductances is observed. Electrical asymmetries in tunnel rates and capacitances must be introduced in order to account for the experimental findings. Fast relaxation of the excited states in the quantum dot have to be assumed, in order to explain the absence of certain structures in the transport spectra.

PACS numbers: 73.63.Kv, 71.10.Pm, 72.25.-b

Since the discovery of the Coulomb blockade effect in semiconductors¹ electronic transport properties of quantum dots have been the subject of continuous interest. The interplay of Coulomb interaction between quantized charges, the spectra of orbital states and the electron spin causes a rich variety of effects in the transport spectra of lateral quantum dots². In an external magnetic field, signatures have been found for transitions between different angular momentum states of the single electron Fock-Darwin spectrum^{3,4}, modified by interaction effects⁵. Effects of the electron spin have been observed, including several transport blocking mechanisms. One of these spin blockades was introduced by Ciorga et al.^{6,7}. Due to spin polarized leads Coulomb peaks show a spin dependent amplitude. This was observed in split gate quantum dots and recently in devices made with local anodic oxidation⁸. In nonlinear measurements negative differential conductance was observed and explained in terms of spin dependent tunneling⁹.

In the present paper, we report results of spin blockade measurements of the linear and nonlinear sequential transport of a 2D quantum dot in a perpendicular magnetic field in comparison with a theoretical model. In the considered parameter region, we confirm results concerning angular momentum and spin blockade effects obtained earlier^{6,7,9}. In particular, we observe the characteristic zig-zag patterns of the linear conductance peaks when varying the magnetic field. The positions and the strengths of the linear conductance peaks show a regular alternating behavior as a function of gate voltage and magnetic field. In the nonlinear transport regime a complicated substructure involving certain transitions to excited states is revealed. A striking bi-modal pattern of positive and negative differential conductance (PDC and NDC) is observed below the $(N + 1) \rightarrow N$ transition line which is the extension of the linear zig-zag pattern. This appears to be associated with a strong depletion of the conductance peaks corresponding to transitions $N \rightarrow (N + 1)$. To study the conditions for obtaining

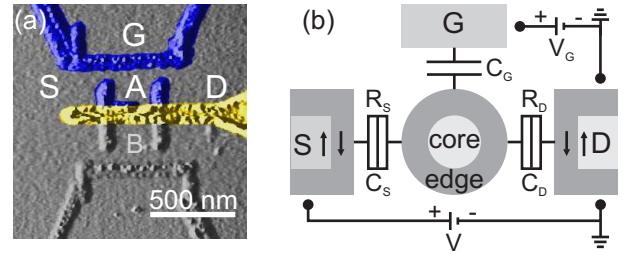


FIG. 1: (a) AFM picture of the gate structures used to define electrostatically a lateral quantum dot in the inversion layer of a AlGaAs/GaAs heterostructure. (b) electrostatic model for the device in a perpendicular magnetic field. The dot with edge and core is coupled via tunnel resistances R and capacitances C to source S and drain D that feature spin split edge channels. The in-plane gate G is coupled capacitively.

the NDC in the nonlinear transport induced by the spin blockade we compare the experimental findings with theoretical results for the nonlinear current-voltage characteristics that were obtained by solving the rate equation for the Fock-Darwin spectrum with suitably defined spin dependent tunnel rates. In addition to the linear conductance we investigated in detail the conditions for the spin induced NDC to appear in the nonlinear differential conductance. It is shown that assuming spin dependent tunneling only is *not* sufficient to understand the data. Our main result is that it is necessary to assume a rather complex interplay of asymmetries, and the *relaxation of certain excited states* to be much faster than the transition rates between leads and core states of the quantum dot, in order to account for the regularity in the experimental conductance traces in a large parameter region.

The quantum dot has been fabricated in an inversion layer embedded in a GaAs/AlGaAs heterostructure. The 2D electron system (2DES) is located 34 nm below the surface. The sheet density is $n = 4.3 \cdot 10^{15} \text{ m}^{-2}$. A combi-

nation of Local Anodic Oxidation (LAO) with an Atomic Force Microscope (AFM) and electron beam lithography (ebeam) is used to define the quantum dot structure visible in Fig. 1a. Details of the sample processing can be found in [10,11]. Quantum dot A is coupled to source (S) and drain (D) leads via resistances R_S and R_D and capacitances C_S and C_D (Fig. 1b). An in-plane gate G is coupled via C_G and can be biased to tune the tunneling rates and electron numbers of the dot. Although the dot B is coupled capacitively to A the measurements discussed here reflect the dynamics of dot A only. They are performed in a regime with dot B only connected to the source lead. Thus transport can occur only via dot A. The influence of the second dot is discussed in [8]. With dot A in the Coulomb blockade regime the differential conductance is recorded using standard lock in technique at a temperature of 50 mK.

Figures 2a,b show typical results for the differential conductance in the plane of V_G and B with $V = 0$. The sawtooth-like traces that are separated by the charging energy show several characteristic features. Firstly, there is a clear *bimodal behavior* of the peak position. An oscillation with a huge increase follows one with a small increase. The same is true for the intensity of the conductance due to spin dependent transport. Secondly, the intensity of all traces with *positive slopes is very weak*, almost not visible in this plot. Thirdly, traces corresponding to successive Coulomb peaks are *shifted relative to each other* by half a period. Large intensities in one trace correspond to small and weak features in the neighboring traces. In the nonlinear conductance (Fig. 2c,d), such features are also present. Additionally, one notes that while the large and strong features are associated with positive differential conductance in the nonlinear region, the smaller and weaker features are continued into the nonlinear regime with NDC. An important observation is that only traces with a *negative slope* as a function of the magnetic field are observed to yield NDC.

In order to understand these features, we consider a model for N uncorrelated electrons in a 2D harmonically confined quantum dot. The ground state energy for N electrons in this system is $H_N = E_C N^2/2 - eNV_G C_G/C_\Sigma - eNV C_S/C_\Sigma + \sum_{j=1}^N \varepsilon_j(B)$. The first term is the classical charge addition energy (E_C charging energy) which accounts for the Coulomb repulsion. $C_\Sigma = C_S + C_D + C_G \approx C_S + C_D$ is the total capacitance of the dot. The lever arm $\alpha = C_G/C_\Sigma$ accounts for the energy change induced by V_G . The last term is the kinetic energy contributed by occupying the energetically lowest one-electron states of the quantum dot with N electrons. The chemical potential for the transition $N - 1 \leftrightarrow N$ is defined as $\mu_N(B) := H_N - H_{N-1} = E_C(N - 1/2) + E_N(B) - eV_G C_G/C_\Sigma - eV C_S/C_\Sigma$. For the nonlinear regime also the lowest lying excited states with energies $H_N^* = H_N + \varepsilon_{N+1} - \varepsilon_N$ must be considered.

For harmonic confinement, $\varepsilon_j(B) = E_j(B) + s_j E_z(B)$ with $E_z = g^* \mu_B B$. The first term represents the j -th level of the Fock-Darwin (FD) spectrum, while the second

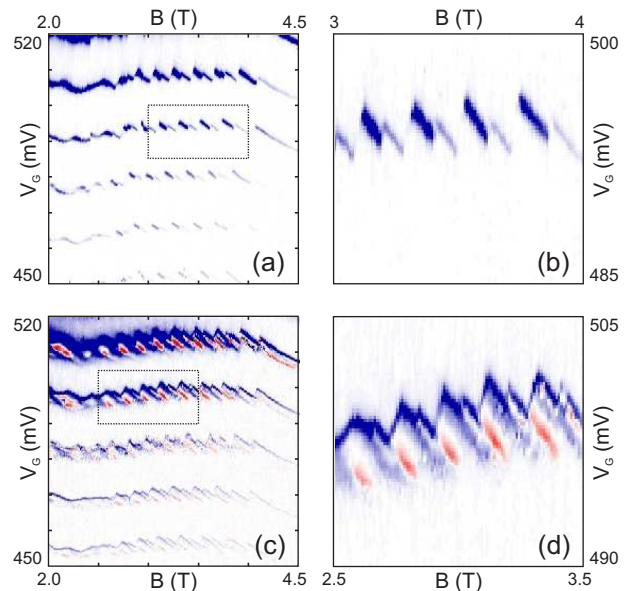


FIG. 2: (a) Linear conductance peaks of the quantum dot in the plane of gate voltage V_G and magnetic field B (dark: high positive differential conductance, bright: low conductance); (b) enlarged inset of (a). The Coulomb peaks develop a bimodal behavior in position and amplitude. (c) spectrum of the nonlinear conductance in the same parameter region at bias $V = 0.5$ mV (red: NDC); (d) enlarged inset of (c). A regular pattern of PDC and NDC is observed.

term describes the Zeeman splitting of the FD spectrum with g^* the electron g -factor, the Bohr magneton μ_B , and $s_j = \pm 1$ the z component of the spin of the j -th FD level (units $\hbar/2$). Here, we assume $\varepsilon_1(B) \leq \varepsilon_2(B) \leq \dots$. For small B , the ground state is a spin singlet or triplet depending on whether N is even or odd, respectively. Increasing the magnetic field, many level-crossings occur in the FD spectrum. This is shown in Fig. 3a where the FD spectrum and the energy level $E_{57}(B)$ are shown for dot filling factor (ν) $2 \leq \nu \leq 4$. For very large magnetic field, $\omega_c = eB/m^* \gg \omega_0$ (m^* electron effective mass, ω_0 characteristic frequency of harmonic confinement potential), the Fock-Darwin levels merge into almost degenerate, Zeeman split Landau bands.

The dot is connected to external noninteracting leads by means of tunneling junctions with resistances $R_{S,D}$ and capacitances $C_{S,D}$ (Fig. 1b). The source (S) terminal is kept at a potential V , while the drain (D) is grounded. At low temperature, for $V > 0$ electrons flow essentially from the drain to the source lead. We consider the tunneling in the sequential regime and introduce the tunneling rates $\Gamma_{i \rightarrow f} \propto \gamma_{i,f} \Gamma_0$ with Γ_0 in dimension of a tunneling rate and $\gamma_{i,f}$ dimensionless parameters which depend on the states involved in the tunneling process. In particular, we have found to be useful to introduce the following parameters: $\gamma_{S,D}$ tunneling via source or drain; $\gamma_{e,c}$ tunneling via edge or core ground state transitions; $\gamma_{e,c}^*$ tunneling via edge or core excited states transitions; $\gamma_{\downarrow,\uparrow}$ tunneling with spin down or spin up. For example,

for tunneling with spin up via the source to an excited state in the core we have $\gamma_{i,f} = \gamma_{\uparrow} \cdot \gamma_S \cdot \gamma_c^*$ (throughout this work, $\gamma_e = 1$, $\gamma_e^* = 1$ and $\gamma_{\downarrow} = 1$).

We have calculated the current and the differential conductance by solving a master equation. First, we address the linear transport regime where only ground states N , $N + 1$ are involved. The transition $N \leftrightarrow N + 1$ occurs if the resonance condition $\mu_{N+1}(B) \approx 0$ is fulfilled. Therefore, the peak position in the plane (B, V_G) reflects the position as a function of B of the $N + 1$ -th energy level. By comparing the linear conductance traces in Fig. 2a and the number of kinks in the trace of the chemical potential in Fig. 3a, one can conclude that the number of electrons is in the range $N = 53, \dots, 57$. In the $2 \leq \nu \leq 4$ regime, the dot states with an increasing (decreasing) $E_j(B)$ have a low (high) angular momentum and are located in the core (edge) of the dot (Fig. 1b). This leads to a weaker (stronger) overlapping of the electron wavefunction with the leads states. To take into account this fact, tunneling rates involving a low angular momentum state are characterized by the factor $0 < \gamma_c < 1$. Moreover, because of the spatial separation of spin-resolved edge states in the leads, tunneling processes involving a state with spin $s_j = +1$ are depressed. We assume that the corresponding rates are renormalized by $0 < \gamma_{\uparrow} < 1$. With these assumptions, the bi-modal behavior can be explained. As shown in Fig. 3b,c where the linear conductance is plotted, lines with positive slopes are strongly suppressed because of the tunneling involving states inside the core of the dot. The lines with a negative slope exhibit a pronounced bi-modal behavior in the intensity, which reflects the alternating spin of the $N + 1$ -th electron in the FD spectrum, Fig. 3a.

At first glance, it might seem that the above assumptions concerning the tunneling rates are quite exhaustive, and should be sufficient to understand also the non-linear behavior at least qualitatively. However, this is not the case, as we have verified by solving the master equation including the states relevant to the nonlinear regime. These are the ground states for N and $N + 1$ electrons as in linear transport and their lowest-lying excited counterparts N^* and $N + 1^*$. For $V > 0$, due to the difference in the chemical potentials of source and drain, the $N \leftrightarrow N + 1$ conductance trace splits, giving rise to "stripes" in the (B, V_G) -plane (Fig. 4a). In addition, new traces due to the transitions $N \leftrightarrow N + 1^*$ and $N^* \leftrightarrow N + 1$ appear. The tunneling rates involving an *excited* state of the dot with low angular momentum are renormalized by the factor $0 < \gamma_c^* < 1$.

To obtain NDC in the upper part of the stripes (Fig. 2d, transitions $N + 1 \rightarrow N$ and $N + 1 \rightarrow N^*$) a tunneling asymmetry $\gamma_S/\gamma_D > 1$ must be assumed, so that the state N^* is dynamically trapped in the dot^{12,13,14} and the current decreases. However, this yields as a function of B traces of conductance peaks with NDC which have both, positive as well as negative slopes (Fig. 4b). In contrast to the experimental findings, the NDC features with positive slopes are even more pronounced than the

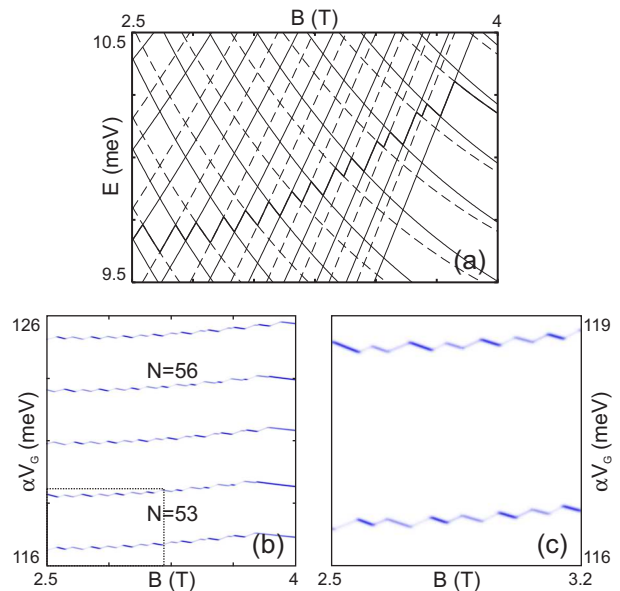


FIG. 3: (a) Fock-Darwin energy spectrum of a quantum dot as a function of the magnetic field B in the $2 \leq \nu \leq 4$ regime: states with spin -1 ($+1$) correspond to solid (dashed) lines; bold: $E_{57}(B)$. (b) Theoretically evaluated linear conductance traces as a function of V_G and B for the transitions $N = 52 \rightarrow 53, \dots, N = 56 \rightarrow 57$ with $\gamma_{\uparrow} = 0.5$ and $\gamma_c = 0.2$ (see text). (c) Enlarged region of (b); parameters: $\hbar\omega_0 = 1.3$ meV, $g^* = 0.44$, $T = 70$ mK.

ones with negative slope. The tunneling suppression due to dot states with low angular momentum enhances the dynamical trapping thus favoring NDC. Moreover, in experiment the transition lines corresponding to transitions $N \rightarrow N + 1$ and $N \rightarrow N + 1^*$ are clearly suppressed.

For a description consistent with the experiment, parameters have to be chosen such that the NDC traces with positive slopes vanish. In addition, the intensity of the lower transition lines must vanish. The former can be achieved assuming $\gamma_c^* < \gamma_c$, and by assuming a strong relaxation of the excited states towards the corresponding ground states. We have introduced a phenomenological relaxation rate $r\Gamma_0$ (r dimensionless constant) into the master equation and consider $r \gg \gamma_c^*$. Then, the relaxation time is much faster than the dwell time of the low angular momentum excited states, leading to a substantial reduction of the NDC. The differential conductance is shown in Fig. 4c. Due to the strong relaxation the conductance exhibits spin-driven bi-modal negative-positive differential conductances in traces with negative slopes, and no NDC in traces with positive slopes.

In order to obtain vanishing conductance peaks in the lower stripes, it is necessary to consider asymmetric capacitances. In Fig. 4d the differential conductance for the same set of parameters as in Fig. 4c is shown, with an asymmetry $C_S/C_D = 1/9$. Qualitative agreement with the experimental findings is obtained.

We have attempted to reproduce theoretically the experimental findings by using many different, physically

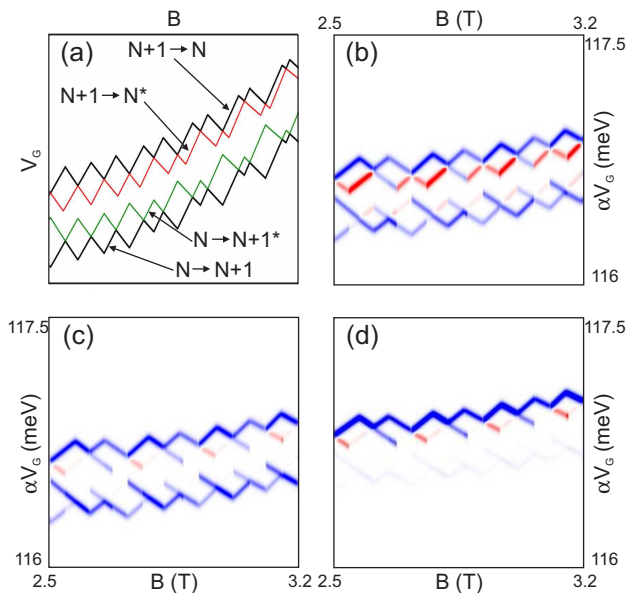


FIG. 4: (a) Scheme of the nonlinear conductance traces in the (B, V_G) plane in the voltage region of the experiment; (b) nonlinear conductance for asymmetric tunnel barriers $\gamma_S/\gamma_D = 50$ and $\gamma_c^* = \gamma_c$ (red: NDC); (c) nonlinear conductance as in (b) with strong relaxation of excited states $r = 1.1$ and $\gamma_c^* = 0.25\gamma_c$; (d) nonlinear conductance as in (c) and asymmetric capacitances $C_S/C_D = 1/9$.

reasonable, combinations of parameters. However, only with the set of parameters discussed here we were successful. Apparently, the patterns of the nonlinear differential conductance traces with the properties shown in Fig. 2 depend very sensitively on the properties of the quantum dot and its environment, in addition to the properties of the tunnel contacts. This has been confirmed experimentally by measuring the nonlinear differential conductance of a different 2D quantum dot. In this case, NDC could not be achieved, although the above discussed bi-modal

features of the linear conductance traces were detected.

In conclusion, we have compared measurements of the nonlinear conductance spectra of 2D quantum dots in a strong perpendicular magnetic field with theoretical current-voltage characteristics obtained by solving a master equation using the Fock-Darwin model together with a set of parameters that characterize the coupling between the quantum dot and the leads, and the properties of the electron states. We have found that in order to reproduce the most prominent features observed experimentally, a rather complex set of model parameters is needed. We have found evidence that it is *not* sufficient to assume spin dependent tunneling. Especially for explaining the regular bi-modal patterns of NDC in the nonlinear conductance it appears to be necessary to assume *fast relaxation of certain excited quantum dot states* in addition to *asymmetry of the tunnel rates*. Furthermore, for reproducing the experimentally observed striking suppression of the traces corresponding to transitions $N \rightarrow (N + 1)$ and $N \rightarrow (N + 1)^*$, asymmetry in source and drain capacitances are necessary.

In contrast to the Coulomb blockade effect, which is universal and independent of the details of the model in the region of sequential tunneling, the spin blockade effect appears not to be universal but very delicately depending on details of the experimental setup. In addition, the experimental data shown in Fig. 2 exhibit features, like the behavior of the slopes of the conductance traces with magnetic field, that apparently cannot be understood within the Fock-Darwin model including the spin. For understanding these features, it appears necessary to take into account electron correlations beyond the constant interaction model.

Financial support by the German BMBF, the European Union via EU-networks, HPRN-CT2000-0144, MCRN-CT2003-504574, and from the Italian MURST PRIN02 is gratefully acknowledged.

¹ U. Meirav, M. A. Kastner, and S. J. Wind, Phys. Rev. Lett. **65**, 771 (1990).
² L. P. Kouwenhoven, C. M. Marcus, P. L. McEuen, S. Tarucha, R. M. Westerveld, and N. S. Wingreen, Mesoscopic Electron Transport, editor G. Schön, Kluwer Dordrecht, volume **345** of Series E, pp. 105-214 (1997).
³ V. Fock, Z. Phys. **47**, 446 (1928).
⁴ C. G. Darwin, Math. Proc. Cambridge Philos. Soc. **27**, 86 (1930).
⁵ P. L. McEuen, E. B. Foxman, J. Kinaret, U. Meirav, M. A. Kastner, N. S. Wingreen, and S. J. Wind. Phys. Rev. B **45**, R11419 (1992).
⁶ M. Ciorga, A. S. Sachrajda, P. Hawrylak, C. Gould, P. Zawadzki, S. Jullian, Y. Feng, and Z. Wasilewski, Phys. Rev. B **61**, R16315 (2000).
⁷ M. Ciorga, A. Wensauer, M. Piore-Ladrière, M. Korkusiński, J. Kyriakidis, A. S. Sachrajda, and P. Hawrylak, Phys. Rev. Lett. **88**, 256804 (2002).

⁸ M. C. Rogge, C. Fühner, U. F. Keyser, R. J. Haug, Appl. Phys. Lett. **85**, 606 (2004).
⁹ M. Ciorga, M. Piore-Ladrière, P. Zawadzki, P. Hawrylak, and A. S. Sachrajda, Appl. Phys. Lett. **80**, 2177 (2002).
¹⁰ M. C. Rogge, C. Fühner, U. F. Keyser, R. J. Haug, M. Bichler, G. Abstreiter, and W. Wegscheider, Appl. Phys. Lett. **83**, 1163 (2003).
¹¹ M. C. Rogge, C. Fühner, U. F. Keyser, M. Bichler, G. Abstreiter, W. Wegscheider, and R. J. Haug, Physica E **21**, 483 (2004).
¹² A. Braggio, M. Sassetti, and B. Kramer, Phys. Rev. Lett. **87**, 146802 (2001).
¹³ F. Cavaliere, A. Braggio, J. T. Stockburger, M. Sassetti, and B. Kramer, Phys. Rev. Lett. **93**, 036803 (2004).
¹⁴ F. Cavaliere, A. Braggio, M. Sassetti, and B. Kramer, Phys. Rev. B **70**, 125323 (2004).